ACS SyntheticBiology

pubs.acs.org/synthbio

Research Article

Engineered L-Lactate Responding Promoter System Operating in Glucose-Rich and Anoxic Environments

Ana Zúñiga, Miguel Camacho, Hung-Ju Chang, Elsa Fristot, Pauline Mayonove, El-Habib Hani, and Jerome Bonnet*

Cite This: *ACS Synth. Biol.* 2021, 10, 3527–3536

Read Online

ACCESS | Metrics & More | Article Recommendations | Supporting Information

ABSTRACT: Bacteria equipped with genetically encoded lactate biosensors are promising tools for biopharmaceutical production, diagnostics, and cellular therapies. However, many applications involve glucose-rich and anoxic environments, in which current whole-cell lactate biosensors show low performance. Here we engineer an optimized, synthetic lactate biosensor system by repurposing the natural LldPRD promoter regulated by the LldR transcriptional regulator. We removed glucose catabolite and anoxic repression by designing a hybrid promoter, containing LldR operators and tuned both regulator and reporter gene expressions to optimize biosensor signal-to-noise ratio. The resulting lactate biosensor, termed ALPaGA (A Lactate Promoter Operating in Glucose and Anoxia), can operate in glucose-rich, aerobic and anoxic conditions. We show that ALPaGA works reliably in the probiotic chassis*Escherichia coli*Nissle 1917 and can detect endogenous L-lactate produced by 3D tumor spheroids with an improved dynamic range. In the future, the ALPaGA system could be used to monitor bioproduction processes and improve the specificity of engineered bacterial cancer therapies by restricting their activity to the lactate-rich microenvironment of solid tumors.

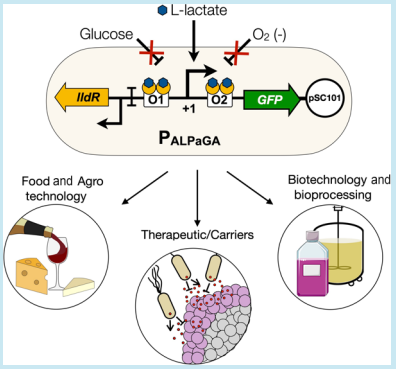

KEYWORDS: *synthetic biology, lactate, whole-cell biosensor, carbon catabolite repression, anoxia, bacterial cancer therapy*

INTRODUCTION

Lactate is an organic acid from alpha-hydroxy acids produced from anaerobic metabolism[1] and has long been considered as a waste end product of cellular metabolism. Lactate can negatively influence the production yield and quality of several bioprocesses, and its monitoring is thus important in food and biopharmaceutical industries.[2−4]

On the other hand, lactate is a versatile and important raw material for various industrial processes. Lactate derivatives are used as food additives for their antimicrobial, antioxidant, or flavoring properties.[5] Lactate is also a basic building block for various biopolymers[6−8] such as polylactic acid used in the construction of biomedical devices because of its biodegradability and biocompatibility.[9] Lactate production is thus an important part of the bioeconomy and is largely produced from renewable feedstocks using the natural sugar fermentation capacity of a wide number of microbes and fungi.[10]

As a central product of anaerobic metabolism, lactate is also a key biomarker of several human physiological states.[1] In medicine, lactic acidosis occurs in several conditions such as sepsis or diabetes and is an important parameter to be monitored in patients admitted in intensive care units.[11] In oncology, lactate produced by cancer cells is a hallmark of solid tumors that leads to tumor acidification and participates in immune system evasion.[12]

For all these reasons, lactate monitoring is highly needed, and several detection systems have been developed.[13−15] Most of them involve enzymatic reactions of lactate oxidase and lactate dehydrogenase coupled to amperometric detection[16] or electrochemical biohybrid oxygen sensing based on natural bacteria metabolism.[17] Yet, these biosensing methods either have low sensitivity or are expensive, limiting their use and deployment. Moreover, these methods are restricted to in vitro applications.

An alternative approach for lactate detection is to use whole-cell biosensors. These sensors are based on living cells, often bacteria, and generally use a specific transcription factor responding to a signal of interest and its target promoter to regulate the expression of a reporter gene.[18,19] This strategy has produced a wide range of biosensors responding to a variety of molecules including glucose, homoserine lactones, heavy metals, butanol, alkanes, and acyl- or malonyl-CoA.[20−29] Whole-cell biosensors are highly sensitive and specific, and the replicating nature of microorganisms supports their cost-

Received: September 17, 2021
Published: December 1, 2021

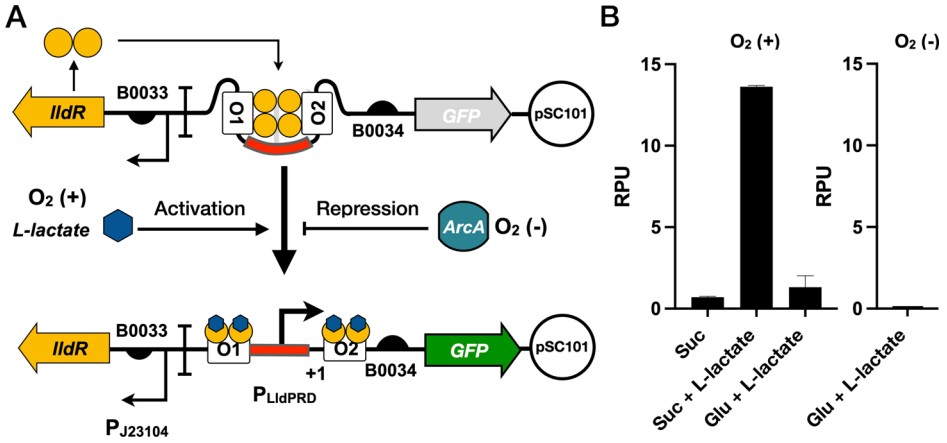

Figure 1. Characterization of the wt LldPRD promoter-based L-lactate biosensor. (A) Architecture and regulation of the low-copy lactate-responsive biosensor based on the wt LldPRD system, repressible in anoxia by ArcA. (B) Response of the wt LldPRD promoter-based L-lactate biosensor to 15 mM succinate, 15 mM succinate plus 10 mM lactate, and 22 mM glucose plus 10 mM lactate under aerobic conditions ($+O_2$) (left) or 22 mM glucose plus 10 mM lactate under anoxia conditions ($-O_2$) (right). Error bars: +/− SD on three biological replicates performed on different days in triplicates. RPU: reference promoter units (see Materials and Methods for details).

Table 1. Functional Analysis of the L-Lactate Biosensor in *E. coli* DH5α[a]

condition	succinate O_2 (+)		glucose O_2 (+)		glucose O_2 (−)	
sensor	PLldPRD	ALPaGA	PLldPRD	ALPaGA	PLldPRD	ALPaGA
leakage RPU	0.8 ± 0.0	1.0 ± 0.1	0.2 ± 0.0	0.9 ± 0.0	0.2 ± 0.0	0.8 ± 0.1
max fold change	13 ± 1.0	8.1 ± 2.0	2.5 ± 0.6	6.2 ± 1.3	1.7 ± 0.1	5.3 ± 1.2
max swing RPU	6.9 ± 0.3	7.0 ± 0.4	0.3 ± 0.0	5.0 ± 0.4	0.1 ± 0.0	3.7 ± 0.1
EC50(M)	1×10^{-3}	9.0×10^{-4}		8.8×10^{-4}		1.1×10^{-3}

[a]RPU: reference promoter units. The leakage RPU corresponds to the RPU in the non-induced state. The max fold change corresponds to the fold change between the induced and non-induced state. The max swing RPU corresponds to the subtraction of RPU between the induced and non-induced state. EC50 is the half-maximal effective concentration in molar. The equation was calculated by using the response function data from three experiments averaged (see the Materials and Methods section). (-: Unable to calculate).

effective production. In addition, genetically encoded sensors can also act as input signals for genetic circuits controlling cellular behavior such as cell growth in specific environmental conditions,[30] conditional control and optimization of metabolic pathways,[31,32] or production and targeted delivery of a therapeutic payload.[33,34]

Genetically encoded lactate biosensors operating in bacteria have been recently engineered, for example, to monitor lactate levels in biopharmaceutical production and to restrain the growth and activity of bacterial cancer therapeutic to the tumor microenvironment.[4,35−37] All these biosensors are based on the *Escherichia coli* LldPRD promoter controlled by the LldR regulator in response to L-lactate[38,39] (Figure 1A). LldR triggers induction of the lldPRD operon responsible for lactate metabolism when *E. coli* cells are grown in lactate as a sole carbon source. Despite having demonstrated the functionality and promising results, the existing lactate biosensors face several challenges.

First, most current lactate biosensors operate on high-copy number plasmids, which are notoriously associated with metabolic burden on the host cell[40,41] and genetic instability,[42] hampering their application both in vitro and in vivo. Biosensors operating at low-copy numbers are thus needed. Second, for many applications, the environment is rich in glucose, the preferred carbon source for *E. coli*[43] which often shuts down the operons controlling the utilization of other carbon sources through carbon catabolite repression (CCR).[44−47] Indeed, the native lactate utilization operon is subject to CCR,[38] and at least, one of the previously engineered lactate biosensors was shown to exhibit a lower performance and an ∼70% lower induction response in the presence of glucose.[4] Third, lactate biosensors would be highly useful in anoxic and micro-oxic environments to monitor lactate production. Indeed, optimal production of lactate is obtained from anaerobically growing lactic acid bacteria[10] which can be mirrored to massive lactate production observed in solid tumors, which is tightly linked to their hypoxic nature.[12] Yet, transcription of the lldPRD operon was shown to be repressed under anoxic conditions by the ArcA protein.[48−52]

Here, we extended the range of applications of L-lactate whole-cell biosensors by engineering and finely tuning its function to perform sensing in glucose-rich and anoxic environments. We characterized this biosensor operating on a low-copy number plasmid in *E. coli* Dh5alpha and Nissle 1917, one of the preferred chassis for therapeutic applications. Finally, we show that ALPaGA can detect endogenous L-lactate produced by 3D tumor spheroids with an improved dynamic range compared to its wild-type version.

RESULTS AND DISCUSSION

We started assessing the functionality of the L-lactate whole-cell biosensor by constructing the one described by Goers and co-workers.[4] This biosensor is based on the wild-type promoter of LldPRD operon and expresses the LldR regulator from the pHyperspank promoter. To address the issues associated with high-copy numbers, we placed this system on a low-copy number plasmid with pSC101 origin of replication

https://doi.org/10.1021/acssynbio.1c00456
ACS Synth. Biol. 2021, 10, 3527−3536

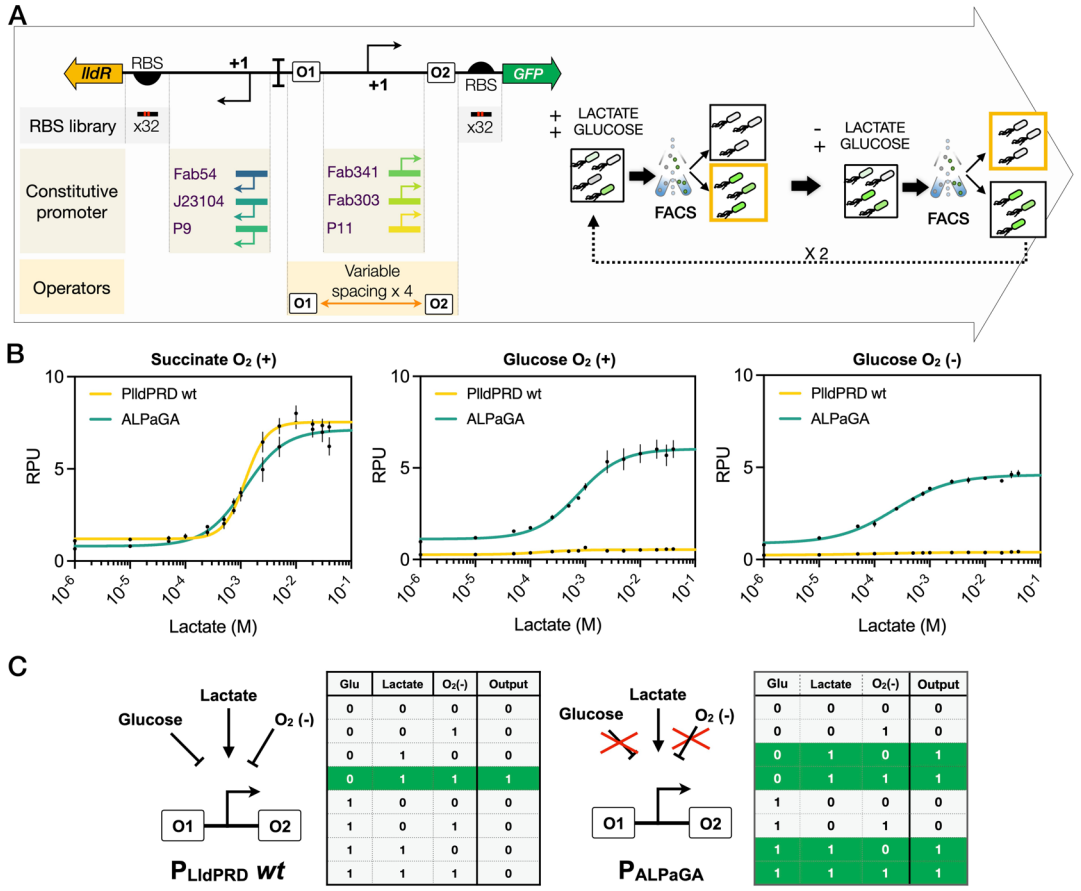

Figure 2. Engineering of an L-lactate whole-cell biosensor operating in a glucose-rich and anoxic environment. (A) Design and optimization of A Lactate Promoter Operating in Glucose and Anoxia, P_{ALPaGA} (left). Design of the synthetic promoter: three different constitutive core promoters, and the two operators were included, varying the original distance from the LldPRD promoter. Three other different promoters were used to control the transcription of the *lldR* regulator. (right) Schematic representation of library screening and enrichment strategy by FACS in M9 plus 22 mM glucose in the presence or absence of 10 mM L-lactate. (B) Response profiles of PlldPRD compared to the engineered ALPaGA sensors to different combinations of lactate, succinate (15 mM), or glucose (22 mM) under aerobic ($+O_2$) or anoxic ($-O_2$) conditions. The fit of the curve was obtained from the mean of three different experiments performed in triplicates on three different days. Error bars: +/− SD. RPU: reference promoter units. Quantified response parameters are summarized in Table 1. (C) Regulatory logic diagram and truth table of the PlldPRD wt and ALPaGA promoter system.

(5−10 copies per chromosome).[53] We designed two other versions of the biosensor in which we used two different strong constitutive promoters to control the expression of the *lldR* gene (Figures 1A and S1A, left). All biosensors were able to sense L-lactate in M9 when lactate was used as a sole carbon source, demonstrating that this system can operate at low-copy numbers (Supporting Information Figure S1A, right), including the control version without the regulator LldR. The versions in which *lldR* expression was driven by strong constitutive promoters (in particular J23104) had a much better response than the one in which pHyperspank was used. The sensor exhibited an ∼13-fold change in accordance with previously published results[37,54] with a half-maximal effective concentration (EC50) of ∼1.1 mM (Figure 1B and Table 1). To assess the sensitivity of the biosensors to CCR, we tested their response in M9 with or without a standard concentration of 22 mM glucose, 43 mM glycerol, or 15 mM succinate. The concentrations of the various carbon sources were chosen to keep a constant number of carbon atoms in the growth media, using as a reference the commonly used glucose concentration. When glucose was added as a carbon source, the biosensor response considerably diminished, confirming strong catabolic repression of the LldPRD promoter by this carbohydrate. In these assays, glycerol negatively affected lactate sensing as compared to the experiments performed in succinate, while glucose totally abolished this response (Figures 1B and S1B,C). Catabolic repression directly affects the LldPRD promoter as repression is observed even when the pHyperspank promoter (also known to be subject to CCR) was not used to control the *lldR* expression. However, we observed that when succinate was used as a carbon source, the pLldPRD promoter was not subjected to CCR (Figures 1B and S1B). We thus used succinate as a non-repressing carbon source in aerobic conditions (and only in those as being an intermediate of oxidative metabolism, succinate cannot be used in anoxic conditions). We then tested the sensor response in anoxic conditions. In agreement with the previous literature,[38,49] we observed no response from the pLldPRD L-lactate biosensor after 16 h of induction, confirming strong inhibition of the promoter (Figures 1B and S1D). These results demonstrate that while being capable of operating at low-copy numbers, the lactate biosensor based on the wild-type LldPRD system is hardly usable in glucose-rich or anoxic conditions, thus greatly limiting its range of applications.

Recently, researchers have built a lactate biosensor based on a hybrid lactate-responsive promoter composed of a weak

https://doi.org/10.1021/acssynbio.1c00456
ACS Synth. Biol. 2021, 10, 3527−3536

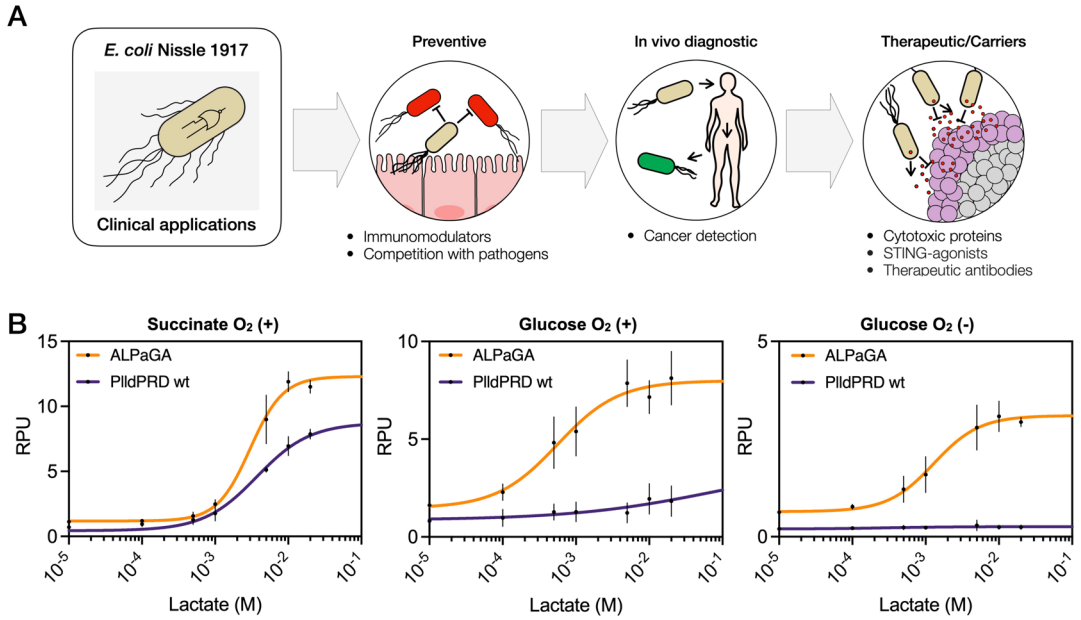

Figure 3. ALPaGA performance in the probiotic strain *E. coli* Nissle 1917. (A) Current summary of the probiotic Nissle 1917 for clinical application. (B) Dose−response functions of the PlldPRD wt biosensor compared to the engineered ALPaGA sensors in different combinations of lactate, succinate, and glucose under aerobic ($+O_2$) or anoxic ($-O_2$) conditions. The fit of the curve was obtained from the mean of three different experiments performed in three different days. Error bars: +/− SD. RPU: reference promoter units. Response parameters are provided in Table 2.

constitutive promoter combined with LldR operators, encapsulated these cells in lipid vesicles, and grew them using glycerol as a carbon source.[35] In this context, this promoter exhibited lower inhibition by glycerol than its wild-type counterpart, suggesting that CCR can be alleviated via promoter engineering approaches. Yet, this promoter was still operating in a high-copy number plasmid and was not fully characterized in glucose-rich or in anoxic conditions. To overcome the repression produced by glucose and anoxia, we thus engineered a synthetic L-lactate promoter exploring an even wider range of sequence parameters and operating in a low-copy number plasmid. This promoter was constructed by using a sequence from a constitutive promoter to replace the sequence between −35 and −10 of the wild-type LldPRD promoter, combined with the operator sequences recognized by LldR. The first version of the system using this synthetic promoter was highly leaky (Figure S2). We thus aimed to optimize the biosensor response through directed evolution by varying the expression of the regulator and the output gene[55] and screening the variants of interest by fluorescence activated cell sorting (FACS). We built a double promoter and RBS library to concomitantly vary the expression of GFP and *lldR* (Figure 2A). All the DNA sequence situated in between operators O1 and O2 of the original LldPRD promoter were replaced (from +1 to the −80), removing the operator sequence for the ArcA repressor, as well as the native −35 and −10 region of the promoter. Of note, we conserved the original operator distance in our new design. The library was transformed into *E. coli* DH5alpha, and FACS sorting was used to screen variants based on GFP fluorescence intensity (Figures 2A and S3). During the first sorting, cells producing GFP were selected after induction with 10 mM L-lactate in the presence of glucose after overnight growth. Thereafter, we performed a negative round of selection without lactate to select variants with lower leakiness. These two rounds were repeated once. Three hundred biosensor variants were recovered and tested for their response to 10 mM lactate and 22 mM glucose in aerobic and anoxic conditions. Variants with higher fold changes were isolated.

We chose the variant with the best fold change in aerobic and anoxic conditions for an additional optimization step, in which we reduced the leakiness of the sensor by placing a weaker RBS sequence (B0033) to control the sfGFP expression. This final biosensor version had an ∼6.2-fold change in the presence of glucose under aerobic conditions and an ∼5.3-fold change in the presence of glucose under anoxic conditions (Table 1). We established a dose−response curve as a function of L-lactate concentration (Figure 2B). The sensor had an EC50 of ∼800 μM under aerobic conditions and ∼1 mM under anoxic conditions (Table 1). These results show that our biosensor can detect L-lactate not only in conditions with high amounts of glucose but also, and importantly, in a limited oxygen context. We termed our system ALPaGA for "A Lactate Promoter Operating in Glucose and Anoxia".

Finally, and as a proof of concept, we aimed at assessing the performance of ALPaGA for L-lactate detection in the tumor microenvironment, a relevant application for bacterial cancer therapy.[56] Since lactate is a major oncometabolite, the use of lactate biosensors has been proposed to restrict the activity or growth of therapeutic bacteria to tumoral tissues and avoid off-target effects, occurring with the majority of anticancer treatments.[54] To evaluate the performance of ALPaGA for tumor-specific control of gene expression, we aimed at sensing endogenous L-lactate produced by tumor spheroids.

Tumor spheroids are relevant in vitro models for tumor cellular response studies[57] and exhibit a gradual accumulation of L-lactate due to the anaerobic metabolism of cells in the internal layers,[58] reproducing hallmark properties of the tumor microenvironment, including oxygen and nutrient gradients.[59] Tumor spheroids represent a challenging and relevant environment to assess the performance of ALPaGA, as the cell culture environment is extremely rich in glucose (25 mM)

https://doi.org/10.1021/acssynbio.1c00456
ACS Synth. Biol. 2021, 10, 3527−3536

Table 2. Functional Analysis of the L-Lactate Biosensor in *E. coli* Nissle 1917[a]

condition	succinate O_2 (+)		glucose O_2 (+)		glucose O_2 (−)	
sensor	PLldPRD	ALPaGA	PLldPRD	ALPaGA	PLldPRD	ALPaGA
leakage RPU	0.5 ± 0.0	1.0 ± 0.0	0.9 ± 0.3	1.4 ± 0.4	0.1 ± 0.0	0.5 ± 0.0
max fold change	7.8 ±0.5	11.8 ± 0.7	1.8 ± 1.3	8.1 ± 2.3	1.4 ± 0.4	5.1 ± 0.3
max swing RPU	6.4 ± 0.6	10.8 ± 0.3	0.8 ± 0.7	6.6 ± 1.4	0.06 ± 0.0	3.8 ± 0.8
EC50(M)	1.7×10^{-3}	1.9×10^{-3}		8.5×10^{-4}		1.2×10^{-3}

[a]RPU: reference promoter units. The leakage RPU corresponds to the RPU in the non-induced state. The max fold change corresponds to the fold change between the induced and non-induced state. The max swing RPU corresponds to the subtraction of RPU between the induced and non-induced state. EC50 is the half-maximal effective concentration in molar. The equation was calculated by using the response function data from three experiments averaged (see Materials and Methods). (-: Unable to calculate).

and the spheroid core becomes rapidly hypoxic. In order to work with a more suitable chassis, we moved our biosensor into the probiotic bacterium *E. coli* Nissle 1917, a strain widely used in diagnostic and therapeutic applications in humans[60−62] (Figure 3A).

The performance of ALPaGA in Nissle 1917 was similar to that observed in Dh5alpha (Figure 3B), presenting an ∼8.1-fold change and an EC50 of ∼800 μM under aerobic conditions and an ∼5.1-fold change and an EC50 of ∼10 mM under anoxic conditions (Table 2).

Before inoculating spheroids with the Nissle 1917 strain, we determined the kinetics of L-lactate production by tumor spheroids. Tumor spheroids were generated using cultured cancerous cells (SW480 colorectal cancer cell line) seeded in ultra-low attachment 96-well plates (Figure 4A), and L-lactate accumulation was measured over 12 days post-seeding in the conditioned medium of cultured spheroids. We found that the L-lactate concentration had a marked increase 6 days post-seeding (Figure 4B), similar to previously reported results.[63,64] Based on these data, we chose to inoculate 7 day-old tumor spheroids with Nissle 1917 harboring either ALPaGA or PLldPRD wt sensors. We observed GFP fluorescence after 24 and 48 h after incubation of the spheroids with ALPaGA sensor but not with the PLldPRD biosensor (Figure 4C). To check if the observed difference in GFP expression within inoculated tumor spheroids between ALPaGA- and PLldPRD-expressing strains was not due to a difference in the colonization ability of each of the two strains, we chromosomally inserted in Nissle 1917 a cassette for constitutively expressing RFP. The strain Nissle 1917:RFP transformed with the L-lactate sensor devices, ALPaGA or PLldPRD, performed similarly to the wt strain (Figures S4 and S5), indicating that there were no metabolic burden effects following RFP insertion.

Next, we inoculated 3D-cultured SW480 spheroids with each of the two sensors and observed their colonization after 48 h by confocal microscopy. While the strain carrying the PLldPRD biosensor colonized the inner layers of SW480 spheroids, no detectable GFP expression was observed (Figure 4D, top). These data were confirmed by flow cytometry analysis of bacteria from spheroid-conditioned medium supernatants, in which no GFP fluorescence was detected (Figure S6). In contrast, a marked expression of GFP by the ALPaGA strains was detected within tumor spheroids after 48 h of co-culture (Figure 4D, bottom). Flow cytometry analysis confirmed that ∼72% of ALPaGA carrying bacteria expressed GFP after 48 h post-inoculation and even 88% after 60 h (Figure S6). Altogether, these results demonstrate that the ALPaGA performance is superior to the wild-type PLldPRD system to detect lactate produced by cancer cells in the context of tumor spheroids. The ALPaGA biosensor may therefore represent a much more suitable biosensor for L-lactate in vivo, particularly in applications aiming at restricting bacterial therapeutic activity and growth to specific locations, such as in the tumor microenvironment.

Here, we describe a novel synthetic lactate biosensor driven by an engineered ALPaGA promoter, which operates reliably in glucose-rich and anoxic conditions, in which previous L-lactate sensor systems using the wild-type LldPRD promoter had poor performance. Importantly, we also show that this biosensor can operate at a low-copy number, excluding unwanted potential metabolic burden effects, making it a better candidate for future research and clinical applications. Indeed, ALPaGA also performed faithfully when implemented in the probiotic model *E. coli* Nissle 1917 and was able to detect lactate in live 3D tumor spheroid models.

In order to generate and optimize ALPaGA, we used a combinatorial tuning method that simultaneously assesses various designer hybrid promoters along with different reporter and transcriptional regulator expression levels by varying their promoter and RBS sequences. We then leveraged FACS to identify and enrich suitable sensors among the thousand variants generated. A previous work aiming at improving the biosensor behavior by tuning the regulator and output expression through RBS and promoter screening used a Small Parts library.[55] On the other hand, FACS-based screening and enrichment was mostly applied to identify new sensors responding to novel ligands.[65−67] Hence, combining these approaches to tune sensor responses allowed us to explore a large parameter space, maximizing our chance to find suitable sensors. The method presented is generalizable and should be useful for tuning the dynamics and signal-to-noise ratio of other transcription-based biosensors.

Although we were able to reduce the biosensor leakiness, ALPaGA still exhibited some marginal background, which may slightly affect its signal-to-noise ratio. Further improvements in biosensor signal-to-noise ratio could thus be made using alternative circuit engineering methods, which have already been applied to the wt LldR system.[37,68] An initial work on LldPRD operon regulation suggested that the distance between the two LldR operators can strongly affect the repression efficiency, which is dependent on DNA looping formed by interacting LldR molecules in the same angular orientation.[38] When we varied the spacing between operators, we observed that by reducing the distance between O2 and −10 in 10 bp, the induction of the system was completely impaired (Figure S7). However, reduction of 10 bp between O1 and −35 did not affect the L-lactate sensing performance. Therefore, while we could not improve the sensor function by manipulating the operator spacing in this study, we cannot exclude that a better

https://doi.org/10.1021/acssynbio.1c00456
ACS Synth. Biol. 2021, 10, 3527−3536

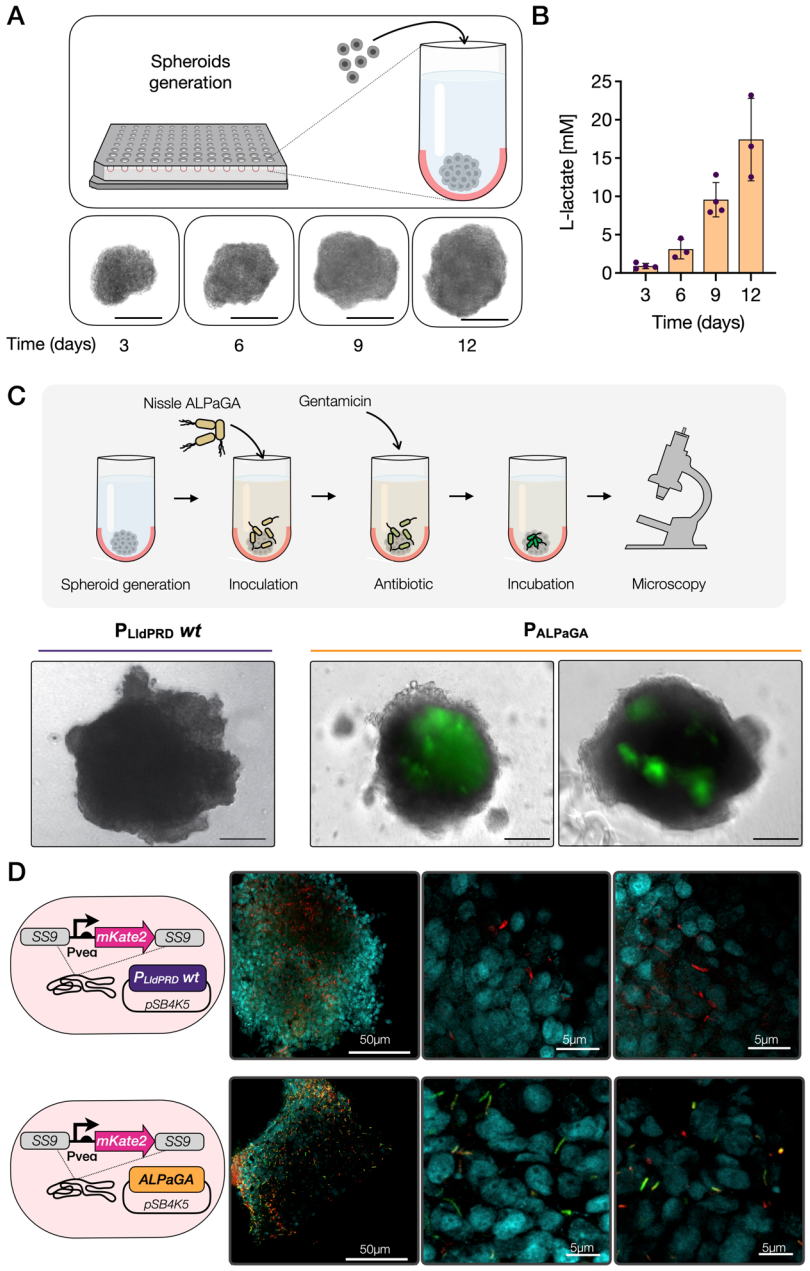

Figure 4. ALPaGA biosensor detecting endogenous lactate in tumor spheroids. (A) Spheroid generation. SW480 cells were seeded on non-adhesive surface plates for spheroid assembly (top). Representative images of tumor SW480 spheroids 3, 6, 9, and 12 days after seed (bottom) from $n = 3$ biological replicates. Scale bars: 100 μm. (B) L-lactate concentration in the medium of SW480 spheroids over 12 days. Bars are the means of three different experiments performed in three different days. Error bars: +/− SD. (C) Nissle 1917-spheroid co-culture. SW480 spheroids were inoculated with PLldPRD wt or ALPaGA for 4 h and were then treated with gentamicin (10 μg/mL) to select bacteria that infiltrated the spheroid. Microscopy analysis was done 48 h post-inoculation (top). Fluorescence microscopy of spheroids colonized by PLldPRD wt (left) or ALPaGA (right) biosensors. Scale bar: 50 μm. (D) Confocal microscopy of spheroids colonized by *E. coli* Nissle 1917:RFP harboring the wt PLldPRD (top) or ALPaGA (bottom) biosensor. Left panels: overlay of DAPI (labeling the DNA in the nucleus of cancer cells), GFP (lactate biosensor response), and RFP (constitutive reporter) fluorescence at 20× magnification. Middle and right panels: representative examples of the response of the lactate biosensors in spheroids at a higher magnification (63×). The samples were fixed 48 h post-inoculation and stained with DAPI before being analyzed by confocal microscopy.

performance could be reached. Replacing the wild-type pLldPRD promoter and the sequence in between both operators allowed us to overcome the repression by glucose and anoxia via ArcA. We determined that the repression observed was not linked to the number of carbon atoms in the medium and was specifically caused by glucose (Figure S8). Yet, the fold change obtained in glucose and anoxia did not reach the same levels as for cells growing in the non-inhibiting carbon source succinate. Thus, other indirect mechanisms repressing the biosensor are suspected to be involved, as previously reported for Crp-mediated catabolite regulation in *E. coli*.[69,70]

Of note, we observed that depending on the strain used, ALPaGA could exhibit a lower fold change than the wt LldPRD system in aerobic and glucose-free conditions (Figures 2B, S4, and S5). Nevertheless, ALPaGA systematically

https://doi.org/10.1021/acssynbio.1c00456
ACS Synth. Biol. 2021, 10, 3527−3536

outperformed the wild-type system in the presence of glucose, with or without oxygen, providing a much more versatile lactate biosensing platform.

The ALPaGA lactate biosensor presented here is of great interest for many applications in which the environment may be glucose rich and/or anoxic, such as monitoring bioproduction processes. The fact that the ALPaGA performance is conserved in Nissle 1917 and that the sensor efficiently detects endogenously produced lactate in tumor spheroids suggests that our biosensor will help improving the current attempts at lactate biosensing to confer a better specificity to bacterial cancer therapy in the context of solid tumors. Future in vivo studies may help confirm the performance and usefulness of the ALPaGA system to fine-tune and specifically guide engineered bacterial cancer therapeutics toward the tumor microenvironment and restrict their activity to this niche.

MATERIALS AND METHODS

Strains and Plasmids. The implementation of the biosensor was done in the *E. coli* strain DH5alphaZ1[71] [laci^q, PN25-tetR, Sp^R, deoR, supE44, Delta (lacZYA-argFV169), Phi80 lacZDeltaM15, hsdR17 (rK− mK+), recA1, endA1, gyrA96, thi-1, and relA1]. For cloning, DH5alphaZ1 was grown on LB medium supplemented with 25 μg/mL kanamycin. For experimental measurements, the cells were grown in M9 minimal medium supplemented with 15 mM succinate or 22 mM glucose or 43 mM glycerol, and 25 μg/mL kanamycin. L-Lactic acid (Sigma-Aldrich, L1750) was used to induce the cells at different concentrations. The ALPaGA plasmid is available from Addgene (plasmid ID: 175272).

Library Design and Plasmid Construction. All the biosensor parts were built on the backbone pSB4K5,[53] containing a pSC101 origin of replication and a kanamycin resistance cassette. The design of the library was made using promoters from the BIOFAB collection (P9, apFAB54, apFAB303, P11, and apFAB341)[72] and the J23104 promoter from the Anderson promoter library (iGEM catalog available at http://parts.igem.org/Promoters/Catalog/Anderson). Sequences are provided in the Supporting Information. The pLldPRD operator sequences were the same as described in ref 37. The RBS library design was derived from the Anderson family with the following sequence: GAAAGACNRGARRC. The ALPaGA promoter library was synthesized as gene fragments purchased from IDT DNA Technologies. Golden Gate was used for DNA assembly.[73] The synthesized DNA fragments were amplified by the Phusion Flash High-Fidelity PCR Master Mix (Thermo Fisher Scientific), purified by using the QIAprep spin Miniprep kit (Qiagen), and digested and ligated overnight. One microgram of the ligation product was transformed into the *E. coli* strain DH5alpha by electroporation. All plasmids were purified using the QIAprep spin Miniprep kit (Qiagen) and sequence-verified by Sanger sequencing (Eurofins Genomics, EU).

To construct the wt PLldPRD biosensor, DNA encoding the LldR transcription factor (lldR) and the wild-type promoter sequence pLldPRD were amplified from the *E. coli* genome based on the previously published design.[4] All primers were designed to support cloning by Gibson assembly at an identical location in the pSB4K5 template vector. All DNA sequences are provided in the Supporting Information.

Sensor Characterization. The different biosensor circuits were transformed into the *E. coli* strain DH5alphaZ1 and plated on LB agar medium containing kanamycin. Three different colonies for each circuit were picked and inoculated, separately, into 500 μL of M9 supplemented with succinate (15 mM) and kanamycin in 96 DeepWell polystyrene plates (Thermo Fisher Scientific, 278606) sealed with an AeraSeal film (Sigma-Aldrich, A9224-50EA) and incubated at 37 °C for 16 h with shaking and 80% humidity in a Kuhner LT-X (Lab-Therm) incubator shaker. After overnight growth, the cells were diluted 1000 times into a fresh M9 minimal medium with antibiotics and L-lactate at different concentrations, with 15 mM succinate, 22 mM glucose, or 43 mM glycerol as indicated. The cells were induced at 37 °C for 16 h with or without shaking for aerobic and anoxic conditions, respectively. Experiments in anoxic conditions were performed by growing the cells in a BD GasPak EZ Anaerobe Container System (BD; 260003) with a BD GasPak EZ pouch system (BD; 260678) for 16 h at 37 °C. Experiments with DH5alphaZ1 were performed without shaking, and experiments on Nissle 1917 with shaking were performed. We verified that shaking DH5alphaZ1 cells in anoxic condition produced similar results for wt pLlPRD and ALPaga sensors (Figure S9). The cells were diluted 200 times in 1× Attune Focusing Fluid (Thermo Fisher Scientific) and kept at room temperature for 1 h before flow cytometry. All experiments were performed in triplicate at three independent occasions.

Flow Cytometry. Flow cytometry was performed on an Attune NxT flow cytometer (Thermo Fisher) equipped with an autosampler and Attune NxT Version 2.7 Software. Experiments on Attune NxT were performed in 96-well plates with setting; FSC: 200 V, SSC: 380 V, and green intensity BL1: 460 V (488 nm laser and 510/10 nm filter). All events were collected with a cutoff of 20,000 events. Every experiment included a negative control with the corresponding plasmid but without the reporter gene to generate the gates. The cells were gated based on forward and side scatter graphs, and events on single-cell gates were selected and analyzed to remove debris from the analysis (Figure S10), by Flow-Jo (Treestar, Inc) software. The geometric mean of the fluorescence was calculated.

Cell Sorting. Cell sorting was performed using a Bio-Rad S3 cell sorter (Bio-Rad). Totally, 100,000 cells were gated under L-lactate and glucose conditions (Figure S3). The cells were collected in SOC medium during the sorting and recovered for 1 h before being inoculated in 10 mL of LB/kanamycin medium for 18 h at 37 °C with shaking.

Data Analysis. Calculation of relative promoter units (RPUs). Fluorescence intensity measurements among different experiments were converted into RPUs by normalizing them according to the fluorescence intensity of the *E. coli* strain DH5alpha containing a reference construct and grown in parallel for each experiment.[74] We used the constitutive promoters J23101 and RBS_B0032 as our in vivo reference standard and placed superfolder GFP as a reporter gene in plasmid pSB4K5. We quantify the geometric mean of fluorescence intensity (MFI) of the flow cytometry data and calculated RPUs according to the following equation

$$\mathrm{RPU} = (\mathrm{MFI}_{\mathrm{sample}})/(\mathrm{MFI}_{\mathrm{reference\ promoter}}) \quad (1)$$

The goodness of fit and the EC50 for each data set were calculated by applying nonlinear regression using the agonist versus response variable slope function in GraphPad Prism. The fold change was calculated as the fluorescence intensity at

https://doi.org/10.1021/acssynbio.1c00456
ACS Synth. Biol. 2021, 10, 3527−3536

maximal lactate concentration divided by the fluorescence intensity without lactate.

SW480 Cell Culture and Spheroid Generation. The human colorectal adenocarcinoma SW480 (CCL-228) cell line used to generate cultured 3D tumor spheroids was obtained from the collection of certified cell lines of the SIRIC Cancer Research Center (http://montpellier-cancer.com/en/le-siric, Montpellier, France). SW480 cells were maintained in culture following standard conditions in the 2D growth mode in Dulbecco's modified Eagle's medium (DMEM, Thermo Fisher) containing 25 mM (0.45% w/v) glucose, supplemented with 2 mM glutamine (Gibco, Thermo Fisher), 1 mM HEPES (Gibco, Thermo Fisher), and 10% ultra-low endotoxin fetal bovine serum (Biowest, Nuaille, France) without antibiotics. To generate 3D spheroids, 2D cultured SW480 cells were passaged using trypsin dissociation and then seeded at a density of 500 cells per 200 μL of culture medium for each well of an ultra-low attachment Nucleon-sphera 96-well plate (Thermo Fisher). The plates were incubated at 37 °C, 5% CO_2, and 95% humidity for at least 7 days before bacteria inoculation was carried out. 3D spheroids usually self-generate by aggregation in low-attaching culture wells within 2−3 h after seeding.

Tumor Spheroid Inoculation. Bacteria harboring the L-lactate biosensor devices were cultured into 500 μL of M9 minimal medium supplemented with 15 mM succinate and kanamycin in 96 DeepWell polystyrene plates (Thermo Fisher Scientific, 278606) sealed with an AeraSeal film (Sigma-Aldrich, A9224-50EA) and incubated at 37 °C for 16 h with shaking and 80% of humidity in a Kuhner LT-X (Lab-Therm) incubator shaker. Cells (10^4 CFU) were inoculated into individual plate wells, each containing an individual 7 day-old SW480 tumor spheroid, which were then returned to the incubator. Six hours after bacterial inoculation, most of the incubation medium was gently discarded, and spheroids were then washed with fresh DMEM three times to remove the initial incubation medium as much as possible (containing residual-free bacteria) without disturbing the spheroids. The medium was replaced with 200 μL of fresh DMEM containing 1.5 μg/mL gentamicin to eliminate any overgrowth of non-colonizing bacteria left at the surface of spheroids.[59] Tumor spheroids were analyzed at 24 and 48 h post-inoculation: The culture medium was removed, and individual spheroids were fixed in 100 μL of 1/10 of 37% paraformaldehyde and stained with DAPI. Fixed spheroids were conserved in tubes with ultrapure Milli-Q water until microscopy analysis.

Fluorescence Microscopy and Confocal Microscopy. Live fluorescence imaging of tumor spheroids was performed using the Evos FL microscope (Thermo Fisher). Pictures were taken with a 4× AMEP4980 objective. Images were acquired at 24, 48 h after L-lactate biosensor inoculation, and analyzed using Fiji software.

Confocal microscopy images were obtained at the Montpellier Ressources Imagerie (MRI) facility. Images were processed at 20×, 40×, or 63× immersion lenses using a Leica SP8 confocal microscope. The excitation wavelengths were 488/581 nm Ex/Em in order to excite GFP, 561/601 Ex/Em for RFP, and 405/444 Ex/Em for DAPI. Images were analyzed with Omero (Open Microscopy Environment) software © 2005−2021.

Measuring L-Lactate Concentration. Lactate production from SW480 spheroids was measured using a L-lactate assay kit (Sigma MAK329). Aliquots of 20 μL of SW480 culture medium were collected from each spheroid-containing well at days 3, 6, 9, and 12 after spheroid seeding. All measurements were performed three times in triplicate in three different days.

■ ASSOCIATED CONTENT

Supporting Information

The Supporting Information is available free of charge at https://pubs.acs.org/doi/10.1021/acssynbio.1c00456.

Characterization of L-lactate biosensors, characterization of the L-lactate promoter, schematics of FACS enrichment, performance comparison of the PLldPRD wt biosensor, performance comparison of the ALPAGA biosensor, cell population analysis, effects of the deletion, effect of equimolar amount of carbon, effect of shaking on biosensors behavior, and gating strategy (PDF)

Raw data (XLSX)

DNA sequence (XLSX)

■ AUTHOR INFORMATION

Corresponding Author

Jerome Bonnet − *Centre de Biologie Structurale (CBS), INSERM U1054, CNRS UMR5048, University of Montpellier, Montpellier 34090, France;* orcid.org/0000-0002-8420-9359; Email: jerome.bonnet@inserm.fr

Authors

Ana Zúñiga − *Centre de Biologie Structurale (CBS), INSERM U1054, CNRS UMR5048, University of Montpellier, Montpellier 34090, France;* orcid.org/0000-0002-2708-0915

Miguel Camacho − *Centre de Biologie Structurale (CBS), INSERM U1054, CNRS UMR5048, University of Montpellier, Montpellier 34090, France*

Hung-Ju Chang − *Centre de Biologie Structurale (CBS), INSERM U1054, CNRS UMR5048, University of Montpellier, Montpellier 34090, France*

Elsa Fristot − *Centre de Biologie Structurale (CBS), INSERM U1054, CNRS UMR5048, University of Montpellier, Montpellier 34090, France*

Pauline Mayonove − *Centre de Biologie Structurale (CBS), INSERM U1054, CNRS UMR5048, University of Montpellier, Montpellier 34090, France*

El-Habib Hani − *Centre de Biologie Structurale (CBS), INSERM U1054, CNRS UMR5048, University of Montpellier, Montpellier 34090, France*

Complete contact information is available at: https://pubs.acs.org/10.1021/acssynbio.1c00456

Author Contributions

A.Z. and J.B. designed the research. A.Z. and H.J.C. designed variant libraries and performed sorting procedures for biosensor optimization by directed evolution. A.Z. and E.F. designed and performed the experiments in anoxic conditions. E.H.H. and P.M. implemented the protocol for spheroid generation. AZ and M.C. performed the experiments of lactate measurement and microscopy. AZ and M.C. performed inoculation of 3D spheroids with the initial help of P.M. and E.H.H. All other experiments were performed by A.Z. A.Z. and J.B. analyzed the data and wrote the article. All authors reviewed and approved the manuscript.

Notes

The authors declare no competing financial interest.

■ ACKNOWLEDGMENTS

We thank the members of the synthetic biology group and of CBS for fruitful discussions and feedback. We thank Béatrice Orsetti, Celine Gongora, and Maggy Del Rio (IRCM, Montpellier) for advice on spheroid generation and the SIRIC for providing SW480 cells. We thank Marie-Pierre Blanchard and Julien Cau from the MRI Platform for help with microscopy. This work was supported by an ERC starting grant "COMPUCELL" and an ANR "SynbioDiag" to J.B. J.B. also acknowledges the INSERM Atip-Avenir program and the Bettencourt-Schueller Foundation for continuous support. CBS acknowledges the support from the French Infrastructure for Integrated Structural Biology (FRISBI) ANR-10-INSB-05-01.

■ REFERENCES

(1) Adeva-Andany, M.; López-Ojén, M.; Funcasta-Calderón, R.; Ameneiros-Rodríguez, E.; Donapetry-García, C.; Vila-Altesor, M.; Rodríguez-Seijas, J. Comprehensive Review on Lactate Metabolism in Human Health. *Mitochondrion* **2014**, *17*, 76−100.

(2) Glacken, M. W.; Fleischaker, R. J.; Sinskey, A. J. Reduction of Waste Product Excretion via Nutrient Control: Possible Strategies for Maximizing Product and Cell Yields on Serum in Cultures of Mammalian Cells. *Biotechnol. Bioeng.* **1986**, *28*, 1376−1389.

(3) Le, H.; Kabbur, S.; Pollastrini, L.; Sun, Z.; Mills, K.; Johnson, K.; Karypis, G.; Hu, W. S. Multivariate analysis of cell culture bioprocess data–lactate consumption as process indicator. *J. Biotechnol.* **2012**, *162*, 210−223.

(4) Goers, L.; Ainsworth, C.; Goey, C. H.; Kontoravdi, C.; Freemont, P. S.; Polizzi, K. M. Whole-cellEscherichia colilactate biosensor for monitoring mammalian cell cultures during biopharmaceutical production. *Biotechnol. Bioeng.* **2017**, *114*, 1290−1300.

(5) Carocho, M.; Morales, P.; Ferreira, I. C. F. R. Antioxidants: Reviewing the Chemistry, Food Applications, Legislation and Role as Preservatives. *Trends Food Sci. Technol.* **2018**, *71*, 107−120.

(6) RedCorn, R.; Engelberth, A. S. Opportunities to Improve the Conversion of Food Waste to Lactate: Fine-Tuning Secondary Factors. *Waste Manag. Res.* **2017**, *35*, 1112−1120.

(7) Castillo Martinez, F. A.; Balciunas, E. M.; Salgado, J. M.; Domínguez González, J. M.; Converti, A.; Oliveira, R. P. d. S. Lactic Acid Properties, Applications and Production: A Review. *Trends Food Sci. Technol.* **2013**, *30*, 70−83.

(8) Abdel-Rahman, M. A.; Tashiro, Y.; Sonomoto, K. Recent Advances in Lactic Acid Production by Microbial Fermentation Processes. *Biotechnol. Adv.* **2013**, *31*, 877−902.

(9) Lasprilla, A. J. R.; Martinez, G. A. R.; Lunelli, B. H.; Jardini, A. L.; Filho, R. M. Poly-lactic acid synthesis for application in biomedical devices - A review. *Biotechnol. Adv.* **2012**, *30*, 321−328.

(10) Juturu, V.; Wu, J. C. Microbial Production of Lactic Acid: The Latest Development. *Crit. Rev. Biotechnol.* **2016**, *36*, 967−977.

(11) Bakker, J.; Nijsten, M. W.; Jansen, T. C. Clinical Use of Lactate Monitoring in Critically Ill Patients. *Ann. Intensive Care* **2013**, *3*, 12.

(12) Morrot, A.; Fonseca, L. M. d.; Salustiano, E. J.; Gentile, L. B.; Conde, L.; Filardy, A. A.; Franklim, T. N.; da Costa, K. M.; Freire-de-Lima, C. G.; Freire-de-Lima, L. Metabolic Symbiosis and Immunomodulation: How Tumor Cell-Derived Lactate May Disturb Innate and Adaptive Immune Responses. *Front. Oncol.* **2018**, *8*, 81.

(13) Rabinowitz, J. D.; Enerbäck, S. Lactate: The Ugly Duckling of Energy Metabolism. *Nat. Metab.* **2020**, *2*, 566−571.

(14) Rassaei, L.; Olthuis, W.; Tsujimura, S.; Sudhölter, E. J. R.; van den Berg, A. Lactate Biosensors: Current Status and Outlook. *Anal. Bioanal. Chem.* **2014**, *406*, 123−137.

(15) Alam, F.; RoyChoudhury, S.; Jalal, A. H.; Umasankar, Y.; Forouzanfar, S.; Akter, N.; Bhansali, S.; Pala, N. Lactate Biosensing: The Emerging Point-of-Care and Personal Health Monitoring. *Biosens. Bioelectron.* **2018**, *117*, 818−829.

(16) Nikolaus, N.; Strehlitz, B. Amperometric Lactate Biosensors and Their Application in (sports) Medicine, for Life Quality and Wellbeing. *Microchim. Acta* **2008**, *160*, 15−55.

(17) Chen, J.; Jin, Y. Sensitive Lactate Determination Based on Acclimated Mixed Bacteria and Palygorskite Co-Modified Oxygen Electrode. *Bioelectrochemistry* **2011**, *80*, 151−154.

(18) Liu, D.; Evans, T.; Zhang, F. Applications and Advances of Metabolite Biosensors for Metabolic Engineering. *Metab. Eng.* **2015**, *31*, 35−43.

(19) Li, L.; Tu, R.; Song, G.; Cheng, J.; Chen, W.; Li, L.; Wang, L.; Wang, Q. Development of a Synthetic 3-Dehydroshikimate Biosensor in Escherichia Coli for Metabolite Monitoring and Genetic Screening. *ACS Synth. Biol.* **2019**, *8*, 297−306.

(20) Shi, S.; Choi, Y. W.; Zhao, H.; Tan, M. H.; Ang, E. L. Discovery and Engineering of a 1-Butanol Biosensor in Saccharomyces Cerevisiae. *Bioresour. Technol.* **2017**, *245*, 1343−1351.

(21) Yu, H.; Chen, Z.; Wang, N.; Yu, S.; Yan, Y.; Huo, Y.-X. Engineering Transcription Factor BmoR for Screening Butanol Overproducers. *Metab. Eng.* **2019**, *56*, 28−38.

(22) Wu, W.; Zhang, L.; Yao, L.; Tan, X.; Liu, X.; Lu, X. Genetically Assembled Fluorescent Biosensor for in Situ Detection of Bio-Synthesized Alkanes. *Sci. Rep.* **2015**, *5*, 10907.

(23) Johnson, A. O.; Gonzalez-Villanueva, M.; Wong, L.; Steinbüchel, A.; Tee, K. L.; Xu, P.; Wong, T. S. Design and Application of Genetically-Encoded Malonyl-CoA Biosensors for Metabolic Engineering of Microbial Cell Factories. *Metab. Eng.* **2017**, *44*, 253−264.

(24) Yang, D.; Kim, W. J.; Yoo, S. M.; Choi, J. H.; Ha, S. H.; Lee, M. H.; Lee, S. Y. Repurposing Type III Polyketide Synthase as a Malonyl-CoA Biosensor for Metabolic Engineering in Bacteria. *Proc. Natl. Acad. Sci. U.S.A.* **2018**, *115*, 9835−9844.

(25) Kim, H. J.; Jeong, H.; Lee, S. J. Synthetic Biology for Microbial Heavy Metal Biosensors. *Anal. Bioanal. Chem.* **2018**, *410*, 1191−1203.

(26) Wan, X.; Volpetti, F.; Petrova, E.; French, C.; Maerkl, S. J.; Wang, B. Cascaded Amplifying Circuits Enable Ultrasensitive Cellular Sensors for Toxic Metals. *Nat. Chem. Biol.* **2019**, *15*, 540−548.

(27) van der Meer, J. R.; Belkin, S. Where Microbiology Meets Microengineering: Design and Applications of Reporter Bacteria. *Nat. Rev. Microbiol.* **2010**, *8*, 511−522.

(28) Courbet, A.; Endy, D.; Renard, E.; Molina, F.; Bonnet, J. Detection of Pathological Biomarkers in Human Clinical Samples via Amplifying Genetic Switches and Logic Gates. *Sci. Transl. Med.* **2015**, *7*, 289ra83.

(29) Kumari, A.; Pasini, P.; Daunert, S. Detection of Bacterial Quorum Sensing N-Acyl Homoserine Lactones in Clinical Samples. *Anal. Bioanal. Chem.* **2008**, *391*, 1619−1627.

(30) Yu, B.; Yang, M.; Shi, L.; Yao, Y.; Jiang, Q.; Li, X.; Tang, L.-H.; Zheng, B.-J.; Yuen, K.-Y.; Smith, D. K.; Song, E.; Huang, J.-D. Explicit Hypoxia Targeting with Tumor Suppression by Creating an "Obligate" Anaerobic Salmonella Typhimurium Strain. *Sci. Rep.* **2012**, *2*, 436.

(31) Skjoedt, M. L.; Snoek, T.; Kildegaard, K. R.; Arsovska, D.; Eichenberger, M.; Goedecke, T. J.; Rajkumar, A. S.; Zhang, J.; Kristensen, M.; Lehka, B. J.; Siedler, S.; Borodina, I.; Jensen, M. K.; Keasling, J. D. Engineering Prokaryotic Transcriptional Activators as Metabolite Biosensors in Yeast. *Nat. Chem. Biol.* **2016**, *12*, 951−958.

(32) Michener, J. K.; Smolke, C. D. High-Throughput Enzyme Evolution in Saccharomyces Cerevisiae Using a Synthetic RNA Switch. *Metab. Eng.* **2012**, *14*, 306−316.

(33) Camacho, E. M.; Mesa-Pereira, B.; Medina, C.; Flores, A.; Santero, E. Engineering Salmonella as Intracellular Factory for Effective Killing of Tumour Cells. *Sci. Rep.* **2016**, *6*, 30591.

(34) Mengesha, A.; Dubois, L.; Lambin, P.; Landuyt, W.; Chiu, R. K.; Wouters, B. G.; Theys, J. Development of a Flexible and Potent Hypoxia-Inducible Promoter for Tumor-Targeted Gene Expression in Attenuated Salmonella. *Cancer Biol. Ther.* **2006**, *5*, 1120−1128.

https://doi.org/10.1021/acssynbio.1c00456
ACS Synth. Biol. 2021, 10, 3527−3536

(35) Trantidou, T.; Dekker, L.; Polizzi, K.; Ces, O.; Elani, Y. Functionalizing Cell-Mimetic Giant Vesicles with Encapsulated Bacterial Biosensors. *Interface Focus* **2018**, *8*, 20180024.
(36) Chien, T.; Harimoto, T.; Kepecs, B.; Gray, K.; Coker, C.; Pu, K.; Azad, T.; Danino, T. *Multiplexed Biosensors for Precision Bacteria Tropism in Vivo*; bioRxiv, 2019, p 851311.
(37) Ho, J. M. L.; Miller, C. A.; Parks, S. E.; Mattia, J. R.; Bennett, M. R. A Suppressor tRNA-Mediated Feedforward Loop Eliminates Leaky Gene Expression in Bacteria. *Nucleic Acids Res.* **2021**, *45*, No. e25.
(38) Aguilera, L.; Campos, E.; Giménez, R.; Badía, J.; Aguilar, J.; Baldoma, L. Dual Role of LldR in Regulation of the lldPRD Operon, Involved in l -Lactate Metabolism in Escherichia coli. *J. Bacteriol.* **2008**, *190*, 2997−3005.
(39) Dong, J. M.; Taylor, J. S.; Latour, D. J.; Iuchi, S.; Lin, E. C. Three Overlapping Lct Genes Involved in L-Lactate Utilization by Escherichia Coli. *J. Bacteriol.* **1993**, *175*, 6671−6678.
(40) Bentley, W. E.; Mirjalili, N.; Andersen, D. C.; Davis, R. H.; Kompala, D. S. Plasmid-encoded protein: The principal factor in the ″metabolic burden″ associated with recombinant bacteria. *Biotechnol. Bioeng.* **1990**, *35*, 668−681.
(41) Birnbaum, S.; Bailey, J. E. Plasmid presence changes the relative levels of many host cell proteins and ribosome components in recombinantEscherichia coli. *Biotechnol. Bioeng.* **1991**, *37*, 736−745.
(42) Jones, S. A.; Melling, J. Persistence of pBR322-Related Plasmids inEscherichia Coligrown in Chemostat Cultures. *FEMS Microbiol. Lett.* **1984**, *22*, 239−243.
(43) Görke, B.; Stülke, J. Carbon Catabolite Repression in Bacteria: Many Ways to Make the Most out of Nutrients. *Nat. Rev. Microbiol.* **2008**, *6*, 613−624.
(44) Postma, P. W.; Lengeler, J. W.; Jacobson, G. R. Phosphoenolpyruvate:carbohydrate Phosphotransferase Systems of Bacteria. *Microbiol. Rev.* **1993**, *57*, 543−594.
(45) Deutscher, J. The Mechanisms of Carbon Catabolite Repression in Bacteria. *Curr. Opin. Microbiol.* **2008**, *11*, 87−93.
(46) Monod, J. The phenomenon of enzymatic adaptation and its bearings on problems of genetics and cellular differentiation. *Molecular Biol.* **1978**, *11*, 68−134.
(47) Epps, H. M.; Gale, E. F. The Influence of the Presence of Glucose during Growth on the Enzymic Activities of Escherichia Coli: Comparison of the Effect with That Produced by Fermentation Acids. *Biochem. J.* **1942**, *36*, 619−623.
(48) Iuchi, S.; Aristarkhov, A.; Dong, J. M.; Taylor, J. S.; Lin, E. C. Effects of Nitrate Respiration on Expression of the Arc-Controlled Operons Encoding Succinate Dehydrogenase and Flavin-Linked L-Lactate Dehydrogenase. *J. Bacteriol.* **1994**, *176*, 1695−1701.
(49) Lynch, A. S.; Lin, E. C. Transcriptional Control Mediated by the ArcA Two-Component Response Regulator Protein of Escherichia Coli: Characterization of DNA Binding at Target Promoters. *J. Bacteriol.* **1996**, *178*, 6238−6249.
(50) Iuchi, S.; Lin, E. C. arcA (dye), a Global Regulatory Gene in Escherichia Coli Mediating Repression of Enzymes in Aerobic Pathways. *Proc. Natl. Acad. Sci. U.S.A.* **1988**, *85*, 1888−1892.
(51) Brückner, R.; Titgemeyer, F. Carbon Catabolite Repression in Bacteria: Choice of the Carbon Source and Autoregulatory Limitation of Sugar Utilization. *FEMS Microbiol. Lett.* **2002**, *209*, 141−148.
(52) Park, D. M.; Akhtar, M. S.; Ansari, A. Z.; Landick, R.; Kiley, P. J. The Bacterial Response Regulator ArcA Uses a Diverse Binding Site Architecture to Regulate Carbon Oxidation Globally. *PLoS Genet.* **2013**, *9*, No. e1003839.
(53) Shetty, R. P.; Endy, D.; Knight, T. F. Engineering BioBrick Vectors from BioBrick Parts. *J. Biol. Eng.* **2008**, *2*, 5.
(54) Chien, T.; Harimoto, T.; Kepecs, B.; Gray, K.; Coker, C.; Hou, N.; Pu, K.; Azad, T.; Nolasco, A.; Pavlicova, M.; Danino, T. Enhancing the Tropism of Bacteria via Genetically Programmed Biosensors. *Nat. Biomed. Eng.* **2021**, *50*, 772.
(55) De Paepe, B.; Maertens, J.; Vanholme, B.; De Mey, M. Modularization and Response Curve Engineering of a Naringenin-Responsive Transcriptional Biosensor. *ACS Synth. Biol.* **2018**, *7*, 1303−1314.
(56) Pawelek, J. M.; Low, K. B.; Bermudes, D. Bacteria as Tumour-Targeting Vectors. *Lancet Oncol.* **2003**, *4*, 548−556.
(57) Ferreira, L. P.; Gaspar, V. M.; Mano, J. F. Design of Spherically Structured 3D in Vitro Tumor Models -Advances and Prospects. *Acta Biomater.* **2018**, *75*, 11−34.
(58) Mehta, G.; Hsiao, A. Y.; Ingram, M.; Luker, G. D.; Takayama, S. Opportunities and Challenges for Use of Tumor Spheroids as Models to Test Drug Delivery and Efficacy. *J. Controlled Release* **2012**, *164*, 192−204.
(59) Harimoto, T.; Singer, Z. S.; Velazquez, O. S.; Zhang, J.; Castro, S.; Hinchliffe, T. E.; Mather, W.; Danino, T. Rapid Screening of Engineered Microbial Therapies in a 3D Multicellular Model. *Proc. Natl. Acad. Sci. U.S.A.* **2019**, *116*, 9002−9007.
(60) Sonnenborn, U.; Schulze, J. The Non-Pathogenic Escherichia Coli Strain Nissle 1917 − Features of a Versatile Probiotic. *Microb. Ecol. Health Dis.* **2009**, *21*, 122−158.
(61) Danino, T.; Prindle, A.; Kwong, G. A.; Skalak, M.; Li, H.; Allen, K.; Hasty, J.; Bhatia, S. N. Programmable Probiotics for Detection of Cancer in Urine. *Sci. Transl. Med.* **2015**, *7*, 289ra84.
(62) Ou, B.; Yang, Y.; Tham, W. L.; Chen, L.; Guo, J.; Zhu, G. Genetic Engineering of Probiotic Escherichia Coli Nissle 1917 for Clinical Application. *Appl. Microbiol. Biotechnol.* **2016**, *100*, 8693−8699.
(63) Bloch, K.; Smith, H.; Hamel Parsons, V.; Gavaghan, D.; Kelly, C.; Fletcher, A.; Maini, P.; Callaghan, R. Metabolic Alterations during the Growth of Tumour Spheroids. *Cell Biochem. Biophys.* **2014**, *68*, 615−628.
(64) Weltin, A.; Hammer, S.; Noor, F.; Kaminski, Y.; Kieninger, J.; Urban, G. A. Accessing 3D Microtissue Metabolism: Lactate and Oxygen Monitoring in Hepatocyte Spheroids. *Biosens. Bioelectron.* **2017**, *87*, 941−948.
(65) Townshend, B.; Kennedy, A. B.; Xiang, J. S.; Smolke, C. D. High-Throughput Cellular RNA Device Engineering. *Nat. Methods* **2015**, *12*, 989−994.
(66) Moser, F.; Espah Borujeni, A.; Ghodasara, A. N.; Cameron, E.; Park, Y.; Voigt, C. A. Dynamic Control of Endogenous Metabolism with Combinatorial Logic Circuits. *Mol. Syst. Biol.* **2018**, *14*, No. e8605.
(67) Tang, S.-Y.; Fazelinia, H.; Cirino, P. C. AraC Regulatory Protein Mutants with Altered Effector Specificity. *J. Am. Chem. Soc.* **2008**, *130*, 5267−5271.
(68) Chen, Y.; Ho, J. M. L.; Shis, D. L.; Gupta, C.; Long, J.; Wagner, D. S.; Ott, W.; Josić, K.; Bennett, M. R. Tuning the Dynamic Range of Bacterial Promoters Regulated by Ligand-Inducible Transcription Factors. *Nat. Commun.* **2018**, *9*, 64.
(69) Gosset, G.; Zhang, Z.; Nayyar, S.; Cuevas, W. A.; Saier, M. H., Jr. Transcriptome Analysis of Crp-Dependent Catabolite Control of Gene Expression in Escherichia Coli. *J. Bacteriol.* **2004**, *186*, 3516−3524.
(70) Lee, D. J.; Minchin, S. D.; Busby, S. J. W. Activating Transcription in Bacteria. *Annu. Rev. Microbiol.* **2012**, *66*, 125−152.
(71) Lutz, R.; Bujard, H. Independent and Tight Regulation of Transcriptional Units in Escherichia Coli via the LacR/O, the TetR/O and AraC/I1-I2 Regulatory Elements. *Nucleic Acids Res.* **1997**, *25*, 1203−1210.
(72) Mutalik, V. K.; Guimaraes, J. C.; Cambray, G.; Lam, C.; Christoffersen, M. J.; Mai, Q.-A.; Tran, A. B.; Paull, M.; Keasling, J. D.; Arkin, A. P.; Endy, D. Precise and Reliable Gene Expression via Standard Transcription and Translation Initiation Elements. *Nat. Methods* **2013**, *10*, 354−360.
(73) Engler, C.; Marillonnet, S. Golden Gate Cloning. *DNA Cloning and Assembly Methods*, 2014; pp 119−131.
(74) Kelly, J. R.; Rubin, A. J.; Davis, J. H.; Ajo-Franklin, C. M.; Cumbers, J.; Czar, M. J.; de Mora, K.; Glieberman, A. L.; Monie, D. D.; Endy, D. Measuring the Activity of BioBrick Promoters Using an in Vivo Reference Standard. *J. Biol. Eng.* **2009**, *3*, 4.

https://doi.org/10.1021/acssynbio.1c00456
ACS Synth. Biol. 2021, 10, 3527−3536